ANTIOXIDANTS & REDOX SIGNALING
Volume 9, Number 10, 2007

DOI: 10.1089/ars.2007.1677

Original Research Communication

On the Biologic Role of the Reaction of NO with Oxidized Cytochrome *c* Oxidase

FERNANDO ANTUNES,[1,2] ALBERTO BOVERIS,[3] and ENRIQUE CADENAS[4]

ABSTRACT

The inhibition of cytochrome *c* oxidase (CcOX) by nitric oxide (NO) is analyzed with a mathematical model that simulates the metabolism *in vivo*. The main results were the following: (a) We derived novel equations for the catalysis of CcOX that can be used to predict CcOX inhibition in any tissue for any [NO] or [O_2]; (b) Competitive inhibition (resulting from the reversible binding of NO to reduced CcOX) emerges has the sole relevant component of CcOX inhibition under state 3 *in vivo*; (c) In state 4, contribution of uncompetitive inhibition (resulting from the reaction of oxidized CcOX with NO) represents a significant nonmajority fraction of inhibition, being favored by high [O_2]; and (d) The main biologic role of the reaction between NO and oxidized CcOX is to consume NO. By reducing [NO], this reaction stimulates, rather than inhibits, respiration. Finally, we propose that the biologic role of NO as an inhibitor of CcOX is twofold: in state 4, it avoids an excessive buildup of mitochondrial membrane potential that triggers rapid production of oxidants, and in state 3, increases the efficiency of oxidative phosphorylation by increasing the ADP/O ratio, supporting the therapeutic use of NO in situations in which mitochondria are dysfunctional. *Antioxid. Redox Signal.* 9, 1569–1579.

INTRODUCTION

Concentrations of NO lower than 100 n*M* control mitochondrial respiration by inhibiting CcOX. Basic features of this inhibition are its competitive character with O_2 and a 50% inhibitory [NO] achieved at low ratios of NO/O_2 (9), which seem to indicate that CcOX has an higher affinity toward NO than toward O_2. Until recently, these characteristics seemed to be at odds with the known and very similar rate constants for the interaction of NO and O_2 with the reduced center of CcOX. In addition, the binding of NO is reversible, whereas O_2 is kinetically trapped. A simple mathematical model showed that this discrepancy is apparent because the catalytic cycle of CcOX works as a dissociation pathway for O_2 (3). This catalytic cycle is faster than the release of NO from the reduced CcOX center, thus explaining the higher apparent affinity of CcOX toward NO.

This model predicted that the degree of inhibition caused by NO depends on how fast the catalytic cycle works: the higher the electron flux, the higher the degree of CcOX inhibition caused by NO. This prediction was later confirmed experimentally (31). In the same set of experiments, it was observed that at low electron fluxes and high O_2 pressures, a deviation occurred from the behavior predicted by the competitive model. This deviation is accounted for by a more complex model that, besides the *reversible binding* of NO to reduced CcOX, also includes the well-known *reaction* of NO with oxidized CcOX, yielding NO_2^-. This reaction causes uncompetitive inhibition

[1]Grupo de Bioquímica dos Oxidantes e Antioxidantes, Centro de Química e Bioquímica and Departamento de Química e Bioquímica, Faculdade de Ciências da Universidade de Lisboa, and [2]Instituto de Investigação Científica Bento da Rocha Cabral, P-1250–047 Lisboa, Portugal.
[3]Laboratory of Free Radical Biology, School of Pharmacy and Biochemistry University of Buenos Aires, Buenos Aires, Argentina.
[4]Department of Pharmacology and Pharmaceutical Sciences, School of Pharmacy, University of Southern California, Los Angeles, California.

[The term noncompetitive, sometimes used to describe this inhibition, is discouraged (1)].

It was concluded that the inhibition of CcOX by NO was a result of both the competitive and the uncompetitive pathways.

Because competitive and uncompetitive inhibition have opposite characteristics concerning the dependence on the electron flux and [O_2] (4, 11, 31) it is important to assess their relative importance, as this will determine the biologic characteristics of CcOX inhibition by NO. A more fundamental biologic question concerns the biologic role of the reaction of NO with oxidized CcOX. Does it increase CcOX inhibition by NO by allowing NO to interact with CcOX across the full *in vivo* ranges of oxygen tension and electron fluxes as proposed (31), or being a reaction that consumes NO, does it act as a safety valve to avoid an excessive CcOX inhibition? In this last scenario, the reaction of CcOX with NO would not only decrease the inhibition of mitochondrial respiration by NO, but it would also control the mitochondrial [NO], with the consequent modulation of NO-dependent signaling events.

To address these fundamental questions, we applied extensive mathematical modeling: (a) Kinetic equations for the inhibition of CcOX by NO, considering simultaneously the competitive and the noncompetitive components were deduced to analyze their relative importance; (b) A model in which NO is simulated as a dynamic variable by including explicitly its synthesis and consumption pathways was set up. Of importance, this model overcomes a key limitation present in previous models, in which [NO] is imposed externally. In the new model, [NO] settles to a steady state that depends on its synthesis and removal as it happens *in vivo*, thus allowing us to study the biologic significance of the removal of NO by its reaction with oxidized CcOX; and (c) this model was *validated* by confronting it with a set of published experimental observations.

The model has predictive value and can be applied to analyze different physiologic or pathologic states in different tissues *in vivo* by changing a few parameters.

MATERIALS AND METHODS

The reactions of the model and respective rate constants are grouped in modules as indicated in Table 1 and shown in Fig. 1. The model was simulated with PLAS (56) or GEPASI (33).

Description of the model

Compartmentation. Compartmentalization was set up as described (2). The basic model contains two compartments that simulate the aqueous mitochondrial matrix and the inner mitochondrial membrane with volumes labeled as V_{aq} and $V_{mitochondrial\ membrane}$, respectively. Suffix "mb" was used to identify species present in the membrane compartment. A value of 5 was assigned to the ratio between the aqueous and membrane compartments. Most reactions in the model occur either

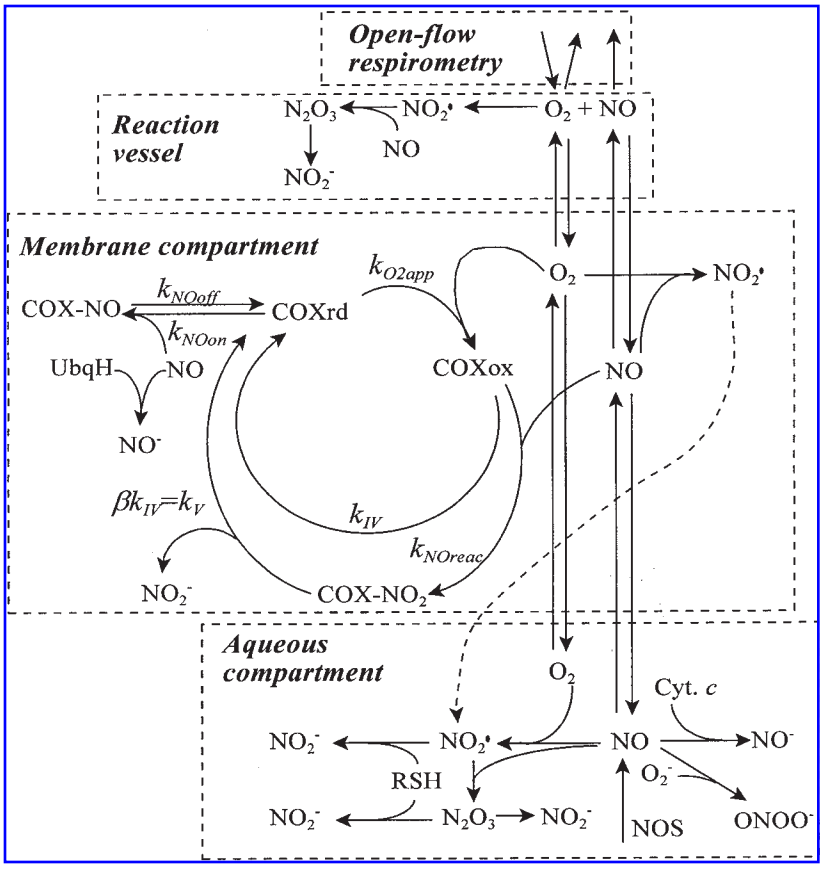

FIG. 1. The reactions included in the mathematical model are grouped in modules. Membrane and aqueous compartments are used to simulate the inhibition of CcOX *in vivo*; the reaction vessel module is added to simulate experiments *in vitro* with mitochondria; simulation of open-flow respirometry experiments needs addition of a set of reactions accounting for the exchange of O_2 and NO with the atmosphere.

TABLE 1. REACTIONS AND PARAMETERS INCLUDED IN THE MATHEMATICAL MODEL

Reaction/species	*Value*	*Reference*
Catalytic cycle of CcOX		
$CcOxrd_{mb} + O_{2mb} \rightarrow CcOXox_{mb} + H_2O$	$k_{O2app} = 1.4 \times 10^8\ M^{-1}$/sec	(3)
$CcOXox_{mb} \rightarrow CcOxrd_{mb}$	$k_{IV} = 7.5$ per sec (state 3)	(3)
	$k_{IV} = 0.75$ per sec (state 4)	(3)
Inhibition of CcOX by NO		
$CcOxrd_{mb} + NO_{mb} \rightarrow NO\text{-}CcOXrd_{mb}$	$k_{NOon} = 1 \times 10^8\ M^{-1}$/sec	
$NO\text{-}CcOXrd_{mb} \rightarrow CcOXrd_{mb} + NO_{mb}$	$k_{NOoff} = 0.01$ per sec	
$CcOxrd_{mb} + NO_{mb} \rightarrow CcOXox - NO_2^-{}_{mb}$	$k_{NOreac} = 2 \times 10^4$ or $2 \times 10^5\ M^{-1}$/sec	(18, 19)
$CcOXox - NO_{2mb} \rightarrow CcOXrd_{mb} + NO_2^-$	0.75 per sec (state 3)	See text
	0.075 per sec (state 4)	
Autoxidation of NO		
$2NO_{mb} + O_{2mb} \rightarrow 2NO_2^{\cdot}$	$2.6 \times 10^7\ M^{-2}$/sec	See text
$2NO + O_2 \rightarrow 2NO_2^{\cdot}$	$6.3 \times 10^6\ M^{-2}$/sec	(23)
$NO + NO_2^{\cdot} \rightarrow N_2O_3$	$1.1 \times 10^9\ M^{-1}$/sec	(20)
$N_2O_3 + H_2O \rightarrow 2NO_2^- + 2H^+$	1.6×10^3 per sec	(29)
$N_2O_3 + RSH \rightarrow NO_2^- + RSNO$	$2.9 \times 10^5\ M^{-1}$/sec	(24)
$NO_2^{\cdot} + RSH \rightarrow NO_2^- + RS + H^+$	$2 \times 10^7\ M^{-1}$/sec	(16)
Other NO-consuming reactions		
$NO_{mb} + UbqH^-{}_{mb} \rightarrow NO^- + Ubq\ \cdot^-{}_{mb} + H^+$	$79.5\ M^{-1}$/sec	See text
$NO + O_2^{\cdot} \rightarrow ONOO^-$	$6.7 \times 10^9\ M^{-1}$/sec	(21)
$Cyt\textit{c}\text{-}Fe^{2+} + NO \rightarrow Cyt\textit{c}\text{-}Fe^{3+} + NO^-$	$2 \times 10^2\ M^{-1}$/sec	(45)
Membrane partition for O_2 and NO		
$O_{2mb} \rightarrow O_2$	1×10^9 per sec	See text
$O_2 \rightarrow O_{2mb}$	3.8×10^9 per sec	See text
$NO_{mb} \rightarrow NO$	1×10^9 per sec	See text
$NO \rightarrow NO_{mb}$	4.4×10^9 per sec	See text
A third compartment that simulates experiments *in vitro*		
$2NO_{out} + O_{2out} \rightarrow 2NO_2{}^{\cdot}{}_{out}$	$6.3 \times 10^6\ M^{-2}$/sec	(23)
$NO_{out} + NO_2{}^{\cdot}{}_{out} \rightarrow N_2O_{3out}$	$1.1 \times 10^9\ M^{-1}$/sec	(20)
$N_2O_{3out} + H_2O \rightarrow 2NO_2^-{}_{out} + 2H^+$	1.6×10^3 per sec	(29)
$O_{2mb} \rightarrow O_{2out}$	1×10^9 per sec	See text
$O_{2out} \rightarrow O_{2mb}$	3.8×10^9 per sec	See text
$NO_{mb} \rightarrow NO_{out}$	1×10^9 per sec	See text
$NO_{out} \rightarrow NO_{mb}$	4.4×10^9 per sec	See text
Open-flow respirometry		
$\rightarrow O_{2out}$	$11.47 \times 10^{-7}\ M$/sec (state 3)	See text
	$3.62 \times 10^{-7}\ M$/sec (state 4)	
$\rightarrow O_{2out}$	0.02 per sec	See text
Species whose concentration is constant with time		
RSH (GSH plus protein thiols)	$5.4 \times 10^{-2}\ M$	(12, 15)
COX_{totmb}	$8.4 \times 10^{-4}\ M$	See text
$Cyt\textit{c}\text{-}Fe^{2+}$	$2 \times 10^{-5}\ M$	(3)
$UbqH^-{}_{mb}$	$1.2 \times 10^{-2}\ M$	See text
$O_2{}^{\cdot}{}^-$	$1 \times 10^{-10}\ M$	(10)
NO, O_2	See figure legends	
Ratios for compartment volumes (V)		
$V_{aq}/V_{mitochondrial\ membrane}$	5	See text
$V_{out}/V_{mitochondria}$[a]	See figure legends	

[a] $V_{mitochondria}$, $V_{aq} + V_{mitochondrial\ membrane}$.

in the membrane phase (reactions involving CcOX and ubiquinol) or in the aqueous phase, but the partition of O_2 and NO between membrane and aqueous phases represents interface reactions in which either O_2 or NO diffuses from one compartment to the other. Rapid equilibriums between NO and O_2 in the two phases were considered. To this end, an arbitrarily high value of 1×10^9 per second was attributed to the membrane-to-aqueous diffusion. Rate constants for the reverse processes were adjusted to obtain partition coefficients between lipid and aqueous phases for O_2 and NO of 3.8 and 4.4, respectively (see Table 1). These values are determined in liposomes (34); the value for NO is lower than the coefficient usually assumed, –9, which is determined in hexane solvent (46). When modeling interface reactions, care must be taken not to violate the mass conservation law. When molecules transfer between compartments with different volumes, the resulting

changes in concentration differ in the respective compartments. We followed the guidelines described (2) for the setting up of these reactions.

To model experiments *in vitro* in which mitochondria suspensions are used, we introduced a third compartment, with volume V_{out}, that simulates the reaction medium in which mitochondria are suspended. We denote species in this compartment by the suffix out. The reactions included were the autoxidation of NO and the partition of O_2 and NO between the external incubation medium and the membrane phase of mitochondria.

Catalytic cycle of CcOX

This set of reactions is based on the minimal model used in ref. 3, in which a single compartment was used because no aqueous reactions were introduced. In this work, we must consider an aqueous compartment, which requires the following adjustment. The original 140 μM for [CcOX] must be multiplied by 6 to convert the concentration units from mitochondrial volume to inner mitochondrial membrane volume. The rate constant for CcOX regeneration is based on a correction of the value used in ref. 3. The original value of 30 per second was based on rates of electron flux per mitochondrial protein. After introducing a stoichiometric factor of four electrons per oxygen molecule, the rate constant decreases by a factor of four, giving 7.5 per second in state 3, and a 10-fold lower value in state 4, as described (3).

Reaction of NO with oxidized CcOX

NO reacts with any of the CcOX intermediates where Cu_B is oxidized, P, F, and O (18, 19, 51), reducing Cu_B. In isolated CcOX, rate constants for the reaction with each of these three intermediates are 8×10^4 M^{-1}/sec for P (18), $(1–2) \times 10^4$ M^{-1}/sec for F (18, 51), and 2×10^5 M^{-1}/sec for O (18). Stoichiometry is 1 with each of these intermediates (18). After this initial reaction, NO is rapidly oxidized to NO_2^- in the CcOX reaction site. We lumped these two reactions into a single step ($CcOX_{ox} + NO \rightarrow CcOX_{ox} - NO_2^-$) with a rate constant in the range 2×10^4 to 2×10^5 M^{-1}/sec. After its formation, NO_2^- is released very slowly from this site, with a time scale of ~1 h, but under turnover conditions, the release is much faster, and the fully reduced center is rapidly regenerated (18, 52). We estimated the rate of this reaction to be 10-fold lower than the regeneration of reduced CcOX in absence of NO, based on the observation that even at very high $[NO_2^-]$, a residual CcOX activity is always present, which has been estimated to be ~10–20% (18, 52).

TABLE 2. RATE LAWS FOR THE INHIBITION OF CcOX BY NO AND FOR THE NO OXIDASE ACTIVITY OF CcOX

	Equation	*Rate law*
1	Competitive linear inhibition	$-\frac{d[O_2]}{dt} = \frac{k_{IV}[COX_{tot}][O_2]}{[O_2] + f_{comp}K_{0.5}}$
2	Uncompetitive hyperbolic inhibition	$-\frac{d[O_2]}{dt} = \frac{k_{IV}[COX_{tot}][O_2]f_{uncomp}}{[O_2] + f_{incomp}K_{0.5}}$
3	Mixed inhibition	$-\frac{d[O_2]}{dt} = \frac{k_{IV}[COX_{tot}][O_2]f_{uncomp}}{[O_2] + f_{comp}f_{uncomp}K_{0.5}}$
4	Eq. 1 = Eq. 2	$[O_2] = \frac{K_{0.5}(K_{0.5NO} + \beta[NO])}{(1-\beta)K_i}$
5	NO oxidase	$-\frac{d[NO]}{dt} = \frac{k_V[COX_{tot}][O_2][NO]}{[O_2][NO] + K_{0.5NO}[O_2] + (\beta K_{0.5}[NO] + K_{0.5}K_{0.5NO})f_{comp}}$

$f_{comp} = \left(1 + \frac{[NO]}{K_i}\right)$; $f_{uncomp} = \left(1 + \beta\frac{[NO]}{K_{0.5NO}}\right) / \left(1 + \frac{[NO]}{K_{0.5NO}}\right)$; $k_V = \beta k_{IV}$; $K_{0.5} = \frac{k_{IV}}{k_{O2app}}$; $K_{0.5NO} = \frac{k_V}{K_{NOreac}}$; $K_i = \frac{k_{NOoff}}{k_{NOon}}$.

Competitive inhibition is caused by the reversible binding of NO to the reduced form of CcOX, whereas uncompetitive inhibition is caused by the reaction of NO with the oxidized form of CcOX. Mixed inhibition is a result of the simultaneous binding and reaction of NO with CcOX. Eq. 4 defines the conditions at which competitive and uncompetitive inhibitions have similar rates. The NO oxidase activity of CcOX corresponds to a two-substrate enzyme under the influence of a competitive inhibitor. Note that $K_{0.5}$ and $K_{0.5NO}$ are not true Michaelis–Menten constants. Meaning of rate constants is indicated in Fig. 1.

NO autoxidation

The autoxidation of NO in the membrane phase is estimated to be 300 times higher than that in the aqueous phase (30). Taking into account the partition coefficients for O_2 and NO between these phases (see earlier), we multiplied the rate constant for the autoxidation in the aqueous phase [6.3×10^6 M^{-2}/sec (23)] by a factor of 4.1, yielding 2.6×10^7 M^{-2}/sec. In this way, a 300-fold higher rate of NO autoxidation in the membrane phase is introduced in the model, as observed experimentally.

Reaction of NO with ubiquinol

The rate constant for the reaction of ubiquinol with NO is estimated to be 2.1×10^3 M^{-1}/sec (42). This estimation has as reference the total mitochondrial volume for the concentration of ubiquinol and the aqueous-phase [NO]. Because in the model we explicitly introduced the mitochondrial inner membrane compartment, we correct this value to $2.1/(6 \times 4.4) \times 10^3$ M^{-1}/sec = 79.5 M^{-1}/sec to account for the ratio of 6 between mitochondria and inner membrane volumes and the partition coefficient of 4.4 between the lipid and aqueous phases for NO.

Concerning the local concentration of ubiquinol, a value of 12 mM for the local concentration was set up, assuming a content of 4 nmol of ubiquinone per milligram of mitochondrial protein (42), a ratio between mitochondria and inner membrane volumes of 6, a volume of mitochondria of 1 μl/mg of mitochondrial protein, and a 50% reduction level for total ubiquinone.

RESULTS

Relative importance of competitive and uncompetitive inhibition

We start by deriving rate equations for competitive, uncompetitive, and mixed inhibition of CcOX by NO. Equation 1 in Table 2 was obtained by us before and corresponds to linear competitive inhibition, in which NO is able to inhibit CcOX fully in competition with O_2 (3). Equation 2 is a novel equation and corresponds to an inhibition type in which NO acts as a hyperbolic uncompetitive inhibitor. It is named hyperbolic because NO is not able to inhibit CcOX fully, which is in accordance with the observed residual activity (10–20%) when measuring cytochrome *c* oxidation starting from the oxidized form of CcOX in the presence of an excess of NO (18, 52). Equation 3 is also a novel equation and includes both types of inhibition simultaneously, yielding a mixed inhibition.

The plot of these equations reveals contrasting characteristics for the various types of inhibition (see Fig. 2). Competitive inhibition decreases for higher [O_2] and increases for higher electron fluxes. Uncompetitive inhibition has the opposite behavior. Inspection of Fig. 1 is helpful to explain these differences:

1. Because of the direct competition between NO and O_2 for the reduced enzyme, it is straightforward that competitive inhibition decreases for higher [O_2]. To react with the oxidized CcOX center, NO needs the previous reaction of CcOX with O_2, so higher [O_2] would *a priori* facilitate uncompetitive inhibition. In general, the increase of the degree of inhibition with substrate concentrations is the hallmark of uncompetitive inhibition (5). Nevertheless, in this case, only a marginal increase is found (Fig. 2a and b) because CcOX is saturated with O_2 to the extent that the reaction of NO with the oxidized center is not limited by O_2.
2. Because the catalytic cycle of CcOX plays the role of a dissociation rate constant for O_2, for higher electron fluxes, the apparent affinity of CcOX toward O_2 decreases, favoring the binding of NO to CcOX in competition with O_2 and, thus, increasing competitive inhibition (3). Uncompetitive inhibition has the opposite dependence on the electron flux (Fig. 2c–e) because the binding of NO to the oxidized enzyme is competing with the

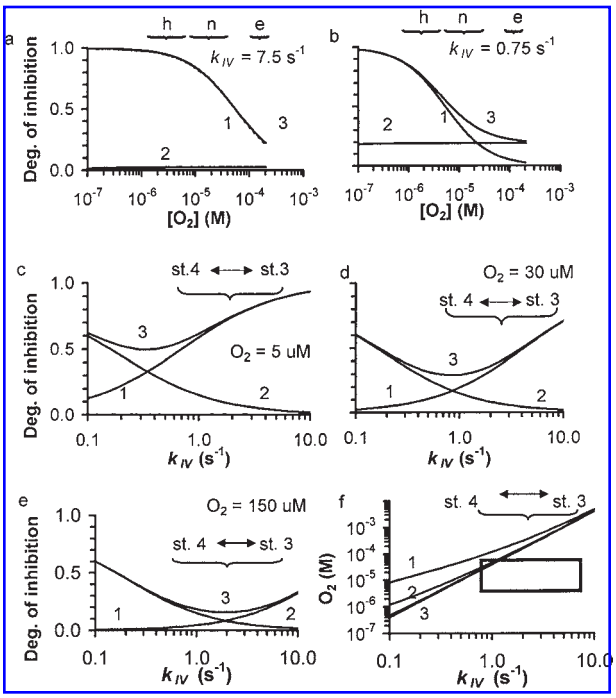

FIG. 2. Relative importance of competitive and uncompetitive components for NO-dependent CcOX inhibition. The degree of CcOX inhibition induced by NO for competitive (1), uncompetitive (2), and mixed (3) inhibition is plotted as a function of [O_2] (**a** and **b**) and CcOX catalytic turnover (k_{IV}; **c–e**). Eqs. 1, 2, and 3 from Table 2 were used to calculate the degree of inhibition. Parameters used are indicated in Table 1; because we used the upper limit for the rate constant for the reaction between oxidized CcOX and NO (k_{NOreac}= 2×10^5 M^{-1}/sec), estimates given are upper limits for the relative importance of the uncompetitive inhibition. In all simulations, [NO] = 100 nM. **a** and **b** simulate states 3 and 4, respectively. [O_2] ranges identified as **h**, **n**, and **e** give approximate ranges for *in vivo* hypoxia, *in vivo* normoxia, and the [O_2] usually applied in experiments *in vitro*, respectively. [O_2] values corresponding to these conditions are studied in detail in **c–e**, in which the electron-flux ranges delimited by states 4 and 3 *in vivo* are indicated. In **f**, Eq. 4 of Table 2 is plotted for [NO] = 10 μM (1), [NO] = 1 μM (2), and [NO] $\leq$ 0.1 μM (3). Lines plotted indicate equal contribution of competitive and uncompetitive component for CcOX inhibition; competitive and uncompetitive inhibition predominates, respectively, below and above each line. Rectangle represents the plausible region for [O_2] and k_{IV} *in vivo*.

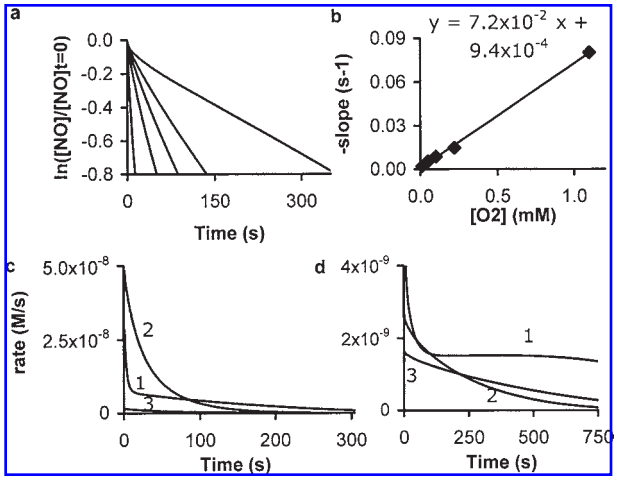

FIG. 3. Simulation of experiments on NO consumption by rat hepatocytes (50). Initial NO added was 3 μM at different $[O_2]$ values. In **a**, a first-order kinetic plot shows the consumption of NO (scale plotted as in ref. 50) for five $[O_2]$ levels. $[O_2]$ values used were 12 μM, 50 μM, 100 μM, 220 μM, and 1.2 mM; the slope increases with the increase of $[O_2]$. In **b**, the slopes of traces in a are plotted, showing a linear correlation with $[O_2]$, which indicates a first-order dependency of NO consumption on $[O_2]$. In **c** and **d**, the pathways removing NO are plotted for $[O_2] = 220$ μM and $[O_2] = 12$ μM, respectively: 1, NO oxidation *via* CcOX; 2, NO autoxidation; 3, Formation of per-oxynitrite. $V_{out}/V_{mitochondria} = 1{,}000$; $k_{IV} = 0.75$ per second $UbqH^- = 0$.

catalytic cycle of the enzyme that regenerates its reduced form. So the higher the electron flux, the lower the reaction of NO with the oxidized site of the enzyme.

Next, we use the equations to predict the relative importance of competitive and uncompetitive inhibition under various conditions. For all $[O_2]$, the competitive component is enough to describe the inhibition of CcOX by NO, if uncoupled state 3 respiration is simulated (see Fig. 2a). The situation is more complex for a low electron flux condition, such as state 4 respiration (see Fig. 2b): in hypoxia, inhibition is competitive; in normoxia, the competitive component prevails, but at the levels applied in typical *in vitro* experiments, the uncompetitive character predominates. This illustrates the misleading character arising from extrapolation from the *in vitro* experiments to the *in vivo* situations. We also predict that for very low electron fluxes (where the affinity of the enzyme toward O_2 is high), the inhibition of the enzyme is almost all accounted for by the uncompetitive component, whereas for high electron fluxes (where the fast turnover outcompetes the reaction of NO with the oxidized enzyme), the competitive component accounts for most of the behavior of the inhibition. The crossing point where both components contribute equally to the overall inhibition is dependent on $[O_2]$: the lower the $[O_2]$, the lower the electron flux where both components contribute equally (see Fig. 2c–e).

The plots shown in Fig. 2a–e were obtained with a [NO] of 100 nM. For [NO] = 25 nM and [NO] = 400 nM, the relative importance of competitive and uncompetitive inhibitions is similar, having similar crossing points (not shown). The better to understand this behavior, we obtained Equation 4 of Table 2, which describes the relation between rate constants $[O_2]$ and [NO], at which competitive and uncompetitive components contribute equally for CcOX inhibition (the crossing points in Fig. 2a–e). For plausible values, $K_{0.5NO} >> \beta$[NO], and so Equation 4 is nearly independent of [NO], as can also be seen in Fig. 2f. NO plays a role on the relative importance of competitive and uncompetitive inhibition only in the micromolar range, and for these, high [NO] competitive inhibition is favored.

Overall, these predictions concur with the experimental observations. In most experiments, the competitive character of the inhibition is observed, whereas the independence of NO inhibition on $[O_2]$ was never reported. The key observation that suggests the importance of the uncompetitive character (*i.e.*, the independence of the rate of NO inhibition reversal on light) was observed under atmospheric conditions at low electron fluxes (32, 44), as predicted in Fig. 2b and e. Recently, the inhibition of CcOX was studied in a wide range of $[O_2]$ and electron fluxes (31): for $[O_2]$ lower than 50 μM the model based solely on the competitive mode fitted well the experimental results (compare with our Fig. 2d). Only for higher $[O_2]$ and low electron fluxes was it necessary to include the uncompetitive mode to have a good fitting with the experimental observations (31) (compare with our Fig. 2e).

Overall, the deduction and plots of the novel equations in Table 2 help establish a rigorous context with which the experimental observations can be compared. It is straightforward with these equations to predict the degree of inhibition and the contribution of the competitive and uncompetitive components by changing the relevant parameters, the $[O_2]$ and [NO] used, and k_{IV} and k_V, which are apparent rate constants that depend on the tissue or CcOX preparations used. With the values used here, which simulate rat liver mitochondria, it can be predicted that *in vivo*, the reaction of NO with oxidized CcOX plays a relevant role for the inhibition of CcOX by NO only for very low electron fluxes.

Mitochondrial catabolism of NO

In the analysis in the previous section, NO was considered a static variable (*i.e.*, it was considered constant over time). This happens in typical experiments in which the effect of a given initial [NO] on the rate of respiration is investigated. *In vivo*, NO changes with time, behaving as a dynamic variable. For example, NO is consumed in the reaction with the oxidized form of CcOX by the rate law described by Equation 5 in Table 2. Thus, by consuming NO, this reaction may stimulate, rather than inhibit, CcOX activity. Note that the reversible binding of NO to the fully reduced CcOX (competitive inhibition) does not consume NO; thus, NO acts as a true inhibitor. To analyze the physiologic role of the reaction between NO and oxidized CcOX, NO must be treated as a dynamic variable.

To perform this analysis, the sinks of NO in mitochondria must be characterized. If a sink outcompetes the reaction of NO with oxidized CcOX, then the consumption of NO *via* CcOX is not significant. However, if the consumption of NO *via* CcOX is the most important mitochondrial NO sink, this reaction will have a key role in [NO] and avoiding an excessive inhibition of CcOX. Unfortunately, the relative importance of pathways consuming NO *in vivo* is not a settled issue, and conflicting evidence favoring different pathways has been presented. There-

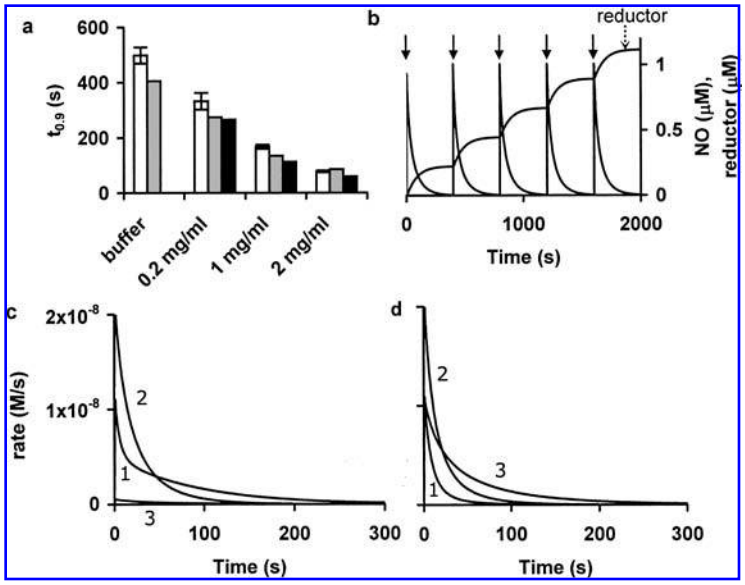

FIG. 4. Simulation of experiments on mitochondrial consumption of NO (49). (**a**) Time needed to consume 90% of a 1-μM initial NO dose ($t_{0.9}$). Presence of mitochondria at 2 mg/ml, 1 mg/ml, 0.2 mg/ml was simulated by setting up a $V_{out}/V_{mitochondria}$ = 500, 1,000, and 5,000, respectively. *White bar*; experimental values taken from (49); *grey bar*, simulation results; *black bar*, simulation results in the presence of respiratory chain inhibitors. Presence of respiratory chain inhibitors was simulated by setting CcOX turnover to zero ($k_{IV} = k_V = 0$ per second; in control, $k_{IV} = 10 \times k_V = 0.75$ per second) and by increasing [$O_2^{\cdot -}$] from 0.1 nM in control to 2.0 nM. The 80% $O_2^{\cdot}$ tension used in ref. 49 was simulated by setting O_2 in aqueous phase to 880 μM. (**b**) Simulation of consecutive additions of NO to mitochondria (*arrows*). $[O_2]_{aqueous\ phase}$ = 990 μM (or 90% O_2 as used in ref. 49); $V_{out}/V_{mitochondria}$ = 1,000; other parameters as in Fig. 3. Reducing equivalents used by CcOX to catabolyze NO are obtained as the integral over time of the rate of NO_2^- release from CcOX and are expressed relative to the overall reaction volume. In **c** and **d**, the pathways removing NO are shown in control conditions and in the presence of respiratory inhibitors, respectively; identification of lines as in Fig. 3.

fore, we include in our model the main reactions that have been proposed as important cellular NO sinks. Besides reaction with CcOX, we included reaction with superoxide, ubiquinols, thiols, and cytochrome *c*, as well as NO autoxidation. To validate this model, we confront it with a set of observations obtained under different experimental conditions that lead to diverse and opposite conclusions concerning NO sinks.

Simulation of experiments in vitro

We started by simulating experiments in which NO consumption by rat hepatocytes is studied as a function of [O_2]. The key finding was that NO consumption is first order on both [NO] and [O_2] (50), which was reproduced by our model (Fig. 3a and b). The negative intercept of the lines of Fig. 3a was also observed experimentally and, according to our model, it is due to a rapid disappearance of NO through reaction with CcOX, forming the CcOX-NO_2 complex. The chemical mechanism explaining the NO decay as a first-order process, both on [O_2] and [NO], is still unknown. According to our model, whereas at high [NO] and high [O_2], autoxidation predominates (Fig. 3c), at low [NO] and low [O_2], NO removal catalyzed by CcOX predominates (Fig. 3d). At intermediate concentrations, the formation of peroxynitrate is also relevant (Fig. 3d). Thus, the apparent first-order NO consumption arises from the sum of all these processes, some of which are not first order, a possibility that had been pointed out originally (50).

Next, we simulated a set of experiments in which the mitochondrial consumption of NO was attributed to the autoxidation of NO in the inner mitochondrial membranes (49). This puzzling conclusion differs from studies in which NO autoxidation was ruled out (50). The key experimental observations that were simulated by our model were (a) NO consumption after addition of 1 μM NO depends on the concentration of mitochondria used (Fig. 4a); (b) respiration inhibitors did not affect significantly the consumption of a single 1-μM dose (Fig. 4a); (c) repeated additions of 1 μM NO were consumed at the same rate (Fig. 4b).

The relative rates of the various pathways that consume NO help us to understand these results. NO autoxidation predominates under the very high O_2 pressures used (Fig. 4c and d), but because the ratio between aqueous and membrane phases is large, this autoxidation occurs in the aqueous phase. For example, at 1 mg/ml of mitochondria, the ratio between total vol-

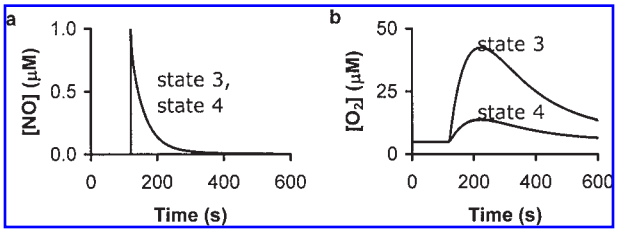

FIG. 5. Simulation of NO consumption by mitochondria under an open-flow respirometry setup (8). [NO] and [O_2] are shown in **a** and **b**, respectively. Before adding NO, O_2 is set up at 5 μM by adjusting the flux of O_2. The basic model was extended to include a module to simulate open-flow respirometry (see Fig. 1). Influx of O_2 was 11.47×10^{-7} M/sec and 3.62×10^{-7} M/sec for states 3 and 4, respectively; experimentally, a flow mixture with 39% or 8% air was used, respectively (8). Removal of NO and O_2 of 0.02 per second was used to have a profile of O_2 removal similar to the experimental one. At 120 sec, [NO] = 1 μM was added. State 3 was simulated with k_{IV} of 7.5 per second, whereas state 4 was simulated with k_{IV} of 1.875 per second to fit the fourfold difference observed experimentally between the rate of respiration in these two states (8). Other parameters as in Fig. 3.

ume and membrane phase is predicted to be 6,000, and so even if the autoxidation in the membrane phase is 300 times faster than in the aqueous phase (30), autoxidation in the aqueous phase is predicted to occur 20-fold faster than that in the lipid phase. On addition of liposomes, the model predicts that for liposome volumes higher than 1/300 of the total reaction volume, autoxidation in the membrane phase outcompetes that in the aqueous phase (not shown), which may explain the increase in the rate of respiration observed experimentally on addition of liposomes (49). If autoxidation in the aqueous phase were the only reaction removing NO, the removal of NO would be independent of the amount of mitochondria. Besides autoxidation, the reaction of NO with oxidized CcOX (in the absence of inhibitors of the respiratory chain) or the reaction of NO with superoxide yielding peroxynitrate (in the presence of inhibitors) contributes significantly to the removal of NO, increasing its importance when [NO] decreases (Fig. 4c and d). These reactions make NO consumption dependent on the amount of mitochondria, explaining the experimental findings. The combined contribution of reactions that need endogenous reductants together with autoxidation also explains why mitochondria are able to consume five consecutive 1-μM NO additions in the absence of respiratory substrates. Only 1.12 μM or 1.12 nmol/mg of protein (assuming 1 μl of mitochondria per mg of protein) reductants is needed for such removal (Fig. 4b). Taking into account the presence of ubiquinone at 5 nmol/mg of protein (42), half of which is expected to be reduced (27), and other partially reduced respiratory complexes, mitochondria seems to be able to catabolize 5 μM NO at the high 90% O_2 used in the experiment, even in the absence of mitochondrial respiratory substrates.

As a final test, we simulated an experiment carried out at levels of O_2 close to 5 μM and under open-flow respirometry (8), conditions that are closer to the *in vivo* situation. The key observation was a similar NO consumption for states 3 and 4 (8). This result was reproduced by the model, and the simulated NO and O_2 time courses were also similar to those observed experimentally (Fig. 5).

In conclusion, apparently contradictory observations may be solely the result of different experimental conditions. Mechanisms revealed to be important under a particular set of experimental conditions may not be relevant under other conditions and may be even irrelevant under conditions *in vivo*. The model presented here reproduced well at a semiquantitative level most of the experimental observations, and therefore, it establishes the basis to predict events *in vivo*.

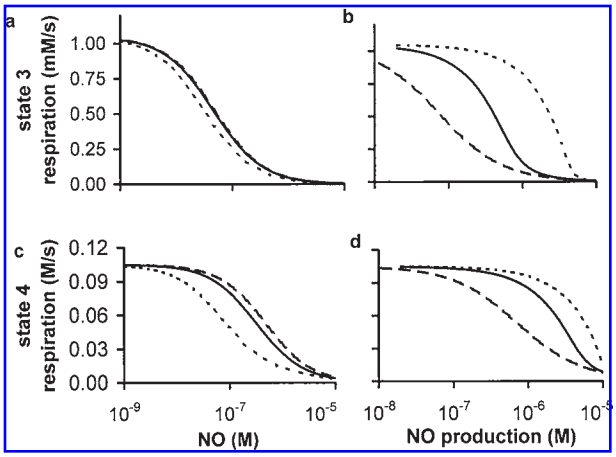

FIG. 7. The reaction of NO with oxidized CcOX (uncompetitive inhibition) stimulates rather than inhibits mitochondrial respiration. Absence of uncompetitive inhibition was simulated by setting the rate constants for the reaction between NO with oxidized CcOX to 0 (– – –); uncompetitive inhibition was simulated at two levels by applying the experimental range of known values for this rate constant, 2×10^4 M^{-1}/sec (——) and 2×10^5 M^{-1}/sec (- - -).

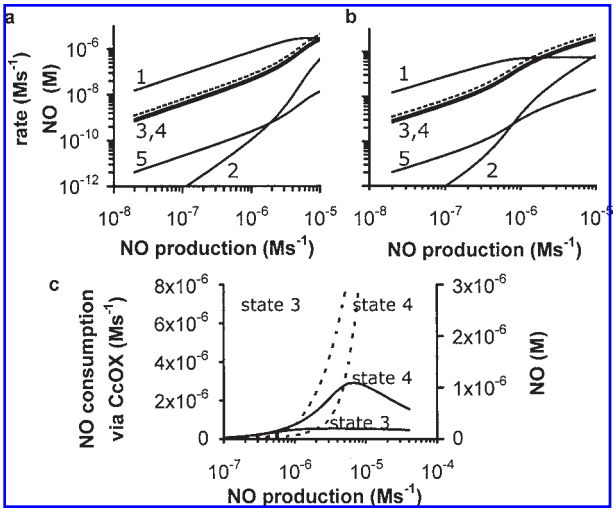

FIG. 6. Simulation of NO sinks *in vivo*. Various pathways consuming NO in mitochondria in states 4 (**a**) and 3 (**b**) as a function of NO production are plotted. [NO] (- - -) and the reaction of NO with CcOX (1), *via* autoxidation (2), with superoxide (3), with ubiquinol (4), and with cytochrome *c* (5) are indicated. (**c**) shows the critical dependence of [NO] (- - -) on NO production when NO consumption *via* CcOX (——) saturates.

Predictions to the state in vivo

In Fig. 6, the relative importance of several consuming NO reactions is compared as a function of NO production. Consumption *via* CcOX predominates by approximately one order of magnitude over the reactions with ubiquinol and superoxide, which have similar orders of magnitude. This is consistent with experiments carried out in cardiomyocytes subjected to endogenous production of NO (between 100 and 150 nM), in which 90% of NO is converted to NO_2^-, involving a mitochondrial component, probably CcOX (22, 37, 39). Note that for higher levels of NO (higher than 0.1 μM in state 3 or higher than 1 μM in state 4), NO consumption by CcOX saturates, and at these levels, [NO] increases sharply (Fig. 6c). Because in state 4, NO consumption *via* CcOX is higher than in state 3, up to fivefold depending on [NO] (Fig. 6c), [NO] in state 4 is lower than in state 3. This prediction holds if NO production is identical in states 3 and 4. Recently, it was found that production of NO *via* the putative mitochondrial NO synthase (mtNOS) (17) is higher in state 4 than in state 3 respiration by ap-

proximately a factor of 2 (53). Figure 6c provides a possible interpretation for the physiologic significance of this finding. A lower NO production in state 3 would delay the onset of a rapid buildup of NO, avoiding an excessive CcOX inhibition. This interpretation is valid only if the main mitochondrial NO source is mtNOS, being the less important contribution of extramitochondrial sources, which is not known so far. The possibility of NO channeling from mtNOS to CcOX because of the physical interaction between mtNOS and CcOX (38) is also relevant. When [NO] increases to such an extent that, because of the competitive inhibition of CcOX *via* NO, CcOX activity is inhibited, the NO consumption *via* CcOX also decreases (see Eq. 5 in Table 2 and Fig. 6c). CcOX inhibition by concentrations of NO in the micromolar range are probably not found *in vivo* because such high [NO] levels are difficult to attain, but it may explain why many experimental setups, in which micromolar [NO] is used, overlook the importance of CcOX as a NO sink. For endogenous NO levels, CcOX emerges as the main sink in the whole cell, even outcompeting myoglobin both in cardiomyocytes *in vitro* (39) and in the myocardium *in vivo* (26).

Next we analyzed the inhibition of respiration by NO *in vivo*. A plot of the inhibition of mitochondrial respiration versus [NO] shows that the reaction of NO with oxidized CcOX (uncompetitive inhibition) is responsible for an increase in CcOX inhibition. This increase is almost negligible in state 3 (Fig. 7a), but more visible in state 4 (Fig. 7c), and conforms to the traditional view of the reaction of NO with oxidized CcOX having an inhibitory effect. This scenario changes if the inhibition of mitochondrial respiration is plotted as a function of the rate of NO production. Now the reaction of NO with CcOX has a stimulatory effect on the mitochondrial respiration both in states 3 (Fig. 7b) and 4 (Fig. 7d). This stimulation comes from the consumption of NO by this reaction. Therefore, under *in vivo* conditions in which [NO] depends on its removal by CcOX, the reaction of CcOX with NO has an effect of avoiding an excessive inhibition of this enzyme by removing the inhibitor from the system.

DISCUSSION

The control exerted by CcOX on mitochondrial respiration is still controversial, but *in vivo*, this control is higher than *in vitro* (40, 55). In this scenario, the inhibition of mitochondrial state 4 respiration by low endogenous [NO] may prevent the buildup of a high membrane potential above the threshold level that triggers the onset of high rates of superoxide production (25). Thus, NO could have an antioxidant effect both by preventing mitochondrial lipid peroxidation triggered by the perhydroxyl radical (6), the protonated form of superoxide, or by avoiding cell damage triggered by the H_2O_2 produced from superoxide dismutation. For lower mitochondrial membrane potentials, endogenous NO may have the opposite effect by increasing the reduction of components of the respiratory chain, triggering a small production of superoxide that could have important regulatory roles (13), including the control of membrane potential *via* uncoupling proteins (14) and synchronization of respiration (7). Independent of the operative membrane potential, the stimulation of mtNOS by the membrane potential (53), the physical interaction of mtNOS with CcOX (38), and the allosteric inhibition of CcOX by ATP (28) are factors that emphasize the inhibitory action of NO in state 4 respiration.

On transition from state 4 to state 3, as CcOX turnover increases, the degree of CcOX inhibition caused by NO also increases (3). Simultaneously, because NO oxidase activity of CcOX is lower in state 3 (Fig. 6c), [NO] increases with this transition. Paradoxically, the system seems to be designed to increase inhibition of respiration when a higher ATP output is needed. As important as the metabolic output is its efficiency. Thus, we propose that NO increases the efficiency of oxidative phosphorylation. Several data support this notion: (a) inhibition of CcOX by azide increases the ADP/O ratio (41); (b) an increase in the ratio between CcOX and the other respiratory complexes decreases the ADP/O ratio (36); whereas (c) a decrease in CcOX protein has the opposite effect (41); (d) endogenous [NO] increases the P/O ratio in guinea pig hearts (47), and (e) decreases heat generation *in vivo* (48); and (f) long-term exposure to NO stimulates mitochondria biogenesis associated with enhanced coupled respiration (35). If the membrane potential decreases, mtNOS decreases production of NO (53), which can lead to a dramatic decrease of [NO] (Fig. 6c), and thus, a higher energetic output, albeit with a lower efficiency, would be possible. These considerations are in agreement with a general role of NO improving metabolic efficiency (43, 57) in which CcOX inhibition by NO in state 3 respiration would play an important role by allowing a higher respiratory coupling (47) and a more efficient delivery of O_2 (50). This view and the role of CcOX as an important NO sink that avoids an excess buildup of NO give mechanistic support to the recent proposal for the therapeutic use of NO for situations in which mitochondria dysfunction is observed, such as obesity (54) and neurodegenerative diseases (35).

ACKNOWLEDGMENTS

This work was supported by grants R01-AG16718 and R-01-ES11342 from the National Institutes of Health to E.C.

ABBREVIATIONS

CcOX, cytochrome *c* oxidase; mtNOS, putative mitochondrial nitric oxide synthase; NO, nitric oxide.

REFERENCES

1. Symbolism and terminology in enzyme kinetics: recommendations 1981. *Biochem J* 213: 561–571, 1983.
2. Alves R, Antunes F, and Salvador A. Tools for kinetic modeling of biochemical networks. *Nat Biotech* 24: 667–672, 2006.
3. Antunes F, Boveris A, and Cadenas E. On the mechanism and biology of cytochrome oxidase inhibition by nitric oxide. *Proc Natl Acad Sci U S A* 101: 16774–16779, 2004.
4. Antunes F and Cadenas E. The mechanism of cytochrome c oxidase inhibition by nitric oxide. *Front Biosci* 12: 975–985, 2007.

5. Antunes F, Marinho HS, Barreto MC, Pavao ML, and Pinto RE. Diagnosis of enzyme inhibition based on the degree of inhibition. *Biochim Biophys Acta* 1624: 11–20, 2003.
6. Antunes F, Salvador A, Marinho HS, Alves R, and Pinto RE. Lipid peroxidation in mitochondrial inner membranes, I. An integrative kinetic model. *Free Radic Biol Med* 21: 917–943, 1996.
7. Aon MA, Cortassa S, Marban E, and O'Rourke B. Synchronized whole cell oscillations in mitochondrial metabolism triggered by a local release of reactive oxygen species in cardiac myocytes. *J Biol Chem* 278: 44735–44744, 2003.
8. Brookes PS, Kraus DW, Shiva S, Doeller JE, Barone MC, Patel RP, Lancaster JR Jr, and Darley-Usmar VM. Control of mitochondrial respiration by no: effects of low oxygen and respiratory state. *J Biol Chem* 278: 31603–31609, 2003.
9. Brown GC. Regulation of mitochondrial respiration by nitric oxide inhibition of cytochrome c oxidase. *Biochim Biophys Acta* 1504: 46–57, 2001.
10. Chance B, Sies H, and Boveris A. Hydroperoxide metabolism in mammalian organs. *Physiol Rev* 59: 527–605, 1979.
11. Cooper CE. Nitric oxide and cytochrome oxidase: substrate, inhibitor or effector? *Trends Biochem Sci* 27: 33–39, 2002.
12. Cotgreave IA, Weis M, Berggren M, Sandy MS, and Moldeus PW. Determination of the intracellular protein thiol distribution of hepatocytes using monobromobimane derivatisation of intact cells and isolated subcellular fractions. *J Biochem Biophys Methods* 16: 247–254, 1988.
13. Demin OV, Kholodenko BN, and Skulachev VP. A model of O2–generation in the complex III of the electron transport chain. *Mol Cell Biochem* 184: 21–33, 1998.
14. Echtay KS, Roussel D, St Pierre J, Jekabsons MB, Cadenas S, Stuart JA, Harper JA, Roebuck SJ, Morrison A, Pickering S, Clapham JC, and Brand MD. Superoxide activates mitochondrial uncoupling proteins. *Nature* 415: 96–99, 2002.
15. Fernandez-Checa J, Garcia R, and Kaplowitz I. Impaired uptake of glutathione by hepatic mitochondria from chronic ethanol-fed rats: tracer kinetics studies in vitro and in vivo and susceptibility to oxidant stress. *J Clin Invest* 87: 397–405, 1991.
16. Ford E, Hughes MN, and Wardman P. Kinetics of the reactions of nitrogen dioxide with glutathione, cysteine, and uric acid at physiological ph. *Free Radic Biol Med* 32: 1314–1323, 2002.
17. Ghafourifar P and Sen CK. Mitochondrial nitric oxide synthase. *Front Biosci* 12: 1072–1078, 2007.
18. Giuffre A, Barone MC, Mastronicola D, D'Itri E, Sarti P, and Brunori M. Reaction of nitric oxide with the turnover intermediates of cytochrome c oxidase: reaction pathway and functional effects. *Biochemistry* 39: 15446–15453, 2000.
19. Giuffre A, Stubauer G, Brunori M, Sarti P, Torres J, and Wilson MT. Chloride bound to oxidized cytochrome c oxidase controls the reaction with nitric oxide. *J Biol Chem* 273: 32475–32478, 1998.
20. Gratzel M, Taniguch S, and Henglein A. Study with pulse radiolysis of no-oxydation and equilibrium N2O3↔NO+NO2 in a water solution. *Ber Buns-Geselsch Phys Chem* 74: 488–492, 1970.
21. Huie R and Padmaja S. The reaction of NO with superoxide. *Free Radic Res Commun* 18: 195–199, 1993.
22. Kanai AJ, Pearce LL, Clemens PR, Birder LA, Vanbibber MM, Choi Sy, De Groat WC, and Peterson J. Identification of a neuronal nitric oxide synthase in isolated cardiac mitochondria using electrochemical detection. *Proc Natl Acad Sci U S A* 98: 14126–14131, 2001.
23. Kharitonov VG, Sundquist AR, and Sharma VS. Kinetics of nitric oxide autoxidation in aqueous solution. *J Biol Chem* 269: 5881–5883, 1994.
24. Kharitonov VG, Sundquist AR, and Sharma VS. Kinetics of nitrosation of thiols by nitric oxide in the presence of oxygen. *J Biol Chem* 270: 28158–28164, 1995.
25. Korshunov SS, Skulachev VP, and Starkov AA. High protonic potential actuates a mechanism of production of reactive oxygen species in mitochondria. *FEBS Lett* 416: 15–18, 1997.
26. Kreutzer U and Jue T. Role of myoglobin as a scavenger of cellular NO in myocardium. *Am J Physiol Heart Circ Physiol* 286: H985–H991, 2004.
27. Lang K, Gohil K, and Packer L. Simultaneous determination of tocopherols, ubiquinols, and ubiquinones in blood, plasma, tissue homogenates, and subcellular fractions. *Anal Biochem* 157: 106–116, 1986.
28. Lee I, Bender E, Arnold S, and Kadenbach B. New control of mitochondrial membrane potential and ROS formation: a hypothesis. *Biol Chem* 382: 1629–1636, 2001.
29. Licht WR and Deen WM. Theoretical-model for predicting rates of nitrosamine and nitrosamide formation in the human stomach. *Carcinogenesis* 9: 2227–2237, 1988.
30. Liu X, Miller MJ, Joshi MS, Thomas DD, and Lancaster JR Jr. Accelerated reaction of nitric oxide with O2 within the hydrophobic interior of biological membranes. *Proc Natl Acad Sci U S A* 95: 2175–2179, 1998.
31. Mason MG, Nicholls P, Wilson MT, and Cooper CE. Nitric oxide inhibition of respiration involves both competitive (heme) and noncompetitive (copper) binding to cytochrome c oxidase. *Proc Natl Acad Sci U S A* 103: 708–713, 2006.
32. Mastronicola D, Genova ML, Arese M, Barone MC, Giuffre A, Bianchi C, Brunori M, Lenaz G, and Sarti P. Control of respiration by nitric oxide in Keilin-Hartree particles, mitochondria and SH-SY5Y neuroblastoma cells. *Cell Mol Life Sci* 60: 1752–1759, 2003.
33. Mendes P. Gepasi: a software package for modelling the dynamics, steady states and control of biochemical and other systems. *Comput Appl Biosci* 9: 563–571, 1993.
34. Moller M, Botti H, Batthyany C, Rubbo H, Radi R, and Denicola A. Direct measurement of nitric oxide and oxygen partitioning into liposomes and low density lipoprotein. *J Biol Chem* 280: 8850–8854, 2005.
35. Nisoli E, Falcone S, Tonello C, Cozzi V, Palomba L, Fiorani M, Pisconti A, Brunelli S, Cardile A, Francolini M, Cantoni O, Carruba MO, Moncada S, and Clementi E. Mitochondrial biogenesis by NO yields functionally active mitochondria in mammals. *Proc Natl Acad Sci U S A* 101: 16507–16512, 2004.
36. Nogueira V, Rigoulet M, Piquet MA, Devin A, Fontaine E, and Leverve XM. Mitochondrial respiratory chain adjustment to cellular energy demand. *J Biol Chem* 276: 46104–46110, 2001.
37. Pearce LL, Kanai AJ, Birder LA, Pitt BR, and Peterson J. The catabolic fate of nitric oxide: the nitric oxide oxidase and peroxynitrite reductase activities of cytochrome oxidase. *J Biol Chem* 277: 13556–13562, 2002.
38. Persichini T, Mazzone V, Polticelli F, Moreno S, Venturini G, Clementi E, and Colasanti M. Mitochondrial type I nitric oxide synthase physically interacts with cytochrome c oxidase. *Neurosci Lett* 384: 254–259, 2005.
39. Peterson J, Kanai AJ, and Pearce LL. A mitochondrial role for catabolism of nitric oxide in cardiomyocytes not involving oxymyoglobin. *Am J Physiol Heart Circ Physiol* 286: H55–H58, 2004.
40. Piccoli C, Scrima R, Boffoli D, and Capitanio N. Control by cytochrome c oxidase of the cellular oxidative phosphorylation system depends on the mitochondrial energy state. *Biochem J* 396: 573–583, 2006.
41. Piquet MA, Nogueira V, Devin A, Sibille B, Filippi C, Fontaine E, Roulet M, Rigoulet M, and Leverve XM. Chronic ethanol ingestion increases efficiency of oxidative phosphorylation in rat liver mitochondria. *FEBS Lett* 468: 239–242, 2000.
42. Poderoso JJ, Lisdero C, Schopfer F, Riobo N, Carreras MC, Cadenas E, and Boveris A. The regulation of mitochondrial oxygen uptake by redox reactions involving nitric oxide and ubiquinol. *J Biol Chem* 274: 37709–37716, 1999.
43. Ruiz-Stewart I, Tiyyagura SR, Lin JE, Kazerounian S, Pitari GM, Schulz S, Martin E, Murad F, and Waldman SA. Guanylyl cyclase is an ATP sensor coupling nitric oxide signaling to cell metabolism. *Proc Natl Acad Sci U S A* 101: 37–42, 2004.
44. Sarti P, Giuffre A, Forte E, Mastronicola D, Barone MC, and Brunori M. Nitric oxide and cytochrome c oxidase: mechanisms of inhibition and no degradation. *Biochem Biophys Res Commun* 274: 183–187, 2000.
45. Sharpe ME and Cooper CE. Reaction of nitric oxide with mitochondrial cytochrome c: a novel mechanism for the formation of nitroxyl anion and peroxynitrite. *Biochem J* 332: 9–19, 1999.
46. Shaw AW and Vosper AJ. Solubility of nitric-oxide in aqueous and non-aqueous solvents. *J Chem Soc Far Trans I* 73: 1239–1244, 1977.

47. Shen W, Tian R, Saupe KW, Spindler M, and Ingwall JS. Endogenous nitric oxide enhances coupling between O2 consumption and ATP synthesis in guinea pig hearts. *Am J Physiol Heart Circ Physiol* 281: H838–H846, 2001.
48. Shen WQ, Xn XB, Ochoa M, Zhao G, Wolin MS, and Hintze TH. Role of nitric-oxide in the regulation of oxygen-consumption in conscious dogs. *Circ Res* 75: 1086–1095, 1994.
49. Shiva S, Brookes PS, Patel RP, Anderson PG, and Darley-Usmar VM. Nitric oxide partitioning into mitochondrial membranes and the control of respiration at cytochrome c oxidase. *Proc Natl Acad Sci U S A* 98: 7212–7217, 2001.
50. Thomas DD, Liu X, Kantrow SP, and Lancaster JR Jr. The biological lifetime of nitric oxide: implications for the perivascular dynamics of NO and O2. *Proc Natl Acad Sci U S A* 98: 355–360, 2001.
51. Torres J, Cooper CE, and Wilson MT. A common mechanism for the interaction of nitric oxide with the oxidized binuclear centre and oxygen intermediates of cytochrome c oxidase. *J Biol Chem* 273: 8756–8766, 1998.
52. Torres J, Sharpe MA, Rosquist A, Cooper CE, and Wilson MT. Cytochrome c oxidase rapidly metabolises nitric oxide to nitrite. *FEBS Lett* 475: 263–266, 2000.
53. Valdez IB, Zaobornyj T, and Boveris A. Mitochondrial metabolic states and membrane potential modulate mtNOS activity. *Biochim Biophys Acta* 1757: 166–172, 2006.
54. Valerio A, Cardile A, Cozzi V, Bracale R, Tedesco L, Pisconti A, Palomba I, Cantoni O, Clementi E, Moncada S, Carruba MO, and Nisoli E. TNF-{alpha} downregulates eNOS expression and mitochondrial biogenesis in fat and muscle of obese rodents. *J Clin Invest* 116: 2791–2798, 2006.
55. Villani G and Attardi G. In vivo control of respiration by cytochrome c oxidase in human cells. *Free Radic Biol Med* 29: 202–210, 2000.
56. Voit E. *Computational analysis of biochemical systems: a practical guide for biochemists and molecular biologists*. Cambridge: Cambridge University Press, 2000.
57. Zhang J, Gong G, Ye Y, Guo T, Mansoor A, Hu Q, Ochiai K, Liu J, Wang X, Cheng Y, Iverson N, Lee J, From AHL, Ugurbil K, and Bache RJ. Nitric oxide regulation of myocardial O2 consumption and HEP metabolism. *Am J Physiol Heart Circ Physiol* 288: H310–H316, 2005.

Address reprint requests to:
Fernando Antunes
Departamento de Química e Bioquímica,
Faculdade de Ciências, Universidade de Lisboa,
P-1749-016 Lisboa,
Portugal

E-mail: fantunes@fc.ul.pt

Date of first submission to ARS Central, April 3, 2007; date of final revised submission, May 14, 2007; date of acceptance, May 21, 2007.

This article has been cited by:

1. Saptarshi Kar, Bhagyesh Bhandar, Mahendra Kavdia. 2012. Impact of SOD in eNOS uncoupling: a two-edged sword between hydrogen peroxide and peroxynitrite. *Free Radical Research* 1-40. [CrossRef]
2. Volker Ullrich , Stefan Schildknecht . Sensing Hypoxia by Mitochondria: A Unifying Hypothesis Involving S-Nitrosation. *Antioxidants & Redox Signaling*, ahead of print. [Abstract] [Full Text HTML] [Full Text PDF] [Full Text PDF with Links]
3. Paula Mariela González, Doris Abele, Susana Puntarulo. 2012. A kinetic approach to assess oxidative metabolism related features in the bivalve Mya arenaria. *Theory in Biosciences* . [CrossRef]
4. Tamara Zaobornyj, Laura Valdez, Alberto BoverisEffect of Sildenafil on Heart Nitric Oxide Metabolism and Mitochondrial Function **30**, 169-188. [CrossRef]
5. Jose Carlos Toledo, Ohara Augusto. 2012. Connecting the Chemical and Biological Properties of Nitric Oxide. *Chemical Research in Toxicology* 120406140527004. [CrossRef]
6. Paolo Sarti, Elena Forte, Daniela Mastronicola, Alessandro Giuffrè, Marzia Arese. 2012. Cytochrome c oxidase and nitric oxide in action: Molecular mechanisms and pathophysiological implications. *Biochimica et Biophysica Acta (BBA) - Bioenergetics* **1817**:4, 610-619. [CrossRef]
7. Virginia Vanasco, Natalia D. Magnani, María Cecilia Cimolai, Laura B. Valdez, Pablo Evelson, Alberto Boveris, Silvia Alvarez. 2012. Endotoxemia impairs heart mitochondrial function by decreasing electron transfer, ATP synthesis and ATP content without affecting membrane potential. *Journal of Bioenergetics and Biomembranes* . [CrossRef]
8. Marzia Arese, Maria Chiara Magnifico, Daniela Mastronicola, Fabio Altieri, Caterina Grillo, Thomas J. J. Blanck, Paolo Sarti. 2012. Nanomolar melatonin enhances nNOS expression and controls HaCaT-cells bioenergetics. *IUBMB Life* n/a-n/a. [CrossRef]
9. Paolo Sarti, Elena Forte, Alessandro Giuffrè, Daniela Mastronicola, Maria Chiara Magnifico, Marzia Arese. 2012. The Chemical Interplay between Nitric Oxide and Mitochondrial Cytochrome c Oxidase: Reactions, Effectors and Pathophysiology. *International Journal of Cell Biology* **2012**, 1-11. [CrossRef]
10. Ricardo M. Santos, Cátia F. Lourenço, Ana Ledo, Rui M. Barbosa, João Laranjinha. 2012. Nitric Oxide Inactivation Mechanisms in the Brain: Role in Bioenergetics and Neurodegeneration. *International Journal of Cell Biology* **2012**, 1-13. [CrossRef]
11. Michelle J. Connolly, Philip I. Aaronson. 2010. Cell redox state and hypoxic pulmonary vasoconstriction: Recent evidence and possible mechanisms#. *Respiratory Physiology & Neurobiology* **174**:3, 165-174. [CrossRef]
12. Ana Navarro, Manuel J. Bández, Carmen Gómez, Marisa G. Repetto, Alberto Boveris. 2010. Effects of rotenone and pyridaben on complex I electron transfer and on mitochondrial nitric oxide synthase functional activity. *Journal of Bioenergetics and Biomembranes* **42**:5, 405-412. [CrossRef]
13. Enara Aguirre, Félix Rodríguez-Juárez, Andrea Bellelli, Erich Gnaiger, Susana Cadenas. 2010. Kinetic model of the inhibition of respiration by endogenous nitric oxide in intact cells. *Biochimica et Biophysica Acta (BBA) - Bioenergetics* **1797**:5, 557-565. [CrossRef]
14. David C. Unitt, Veronica S. Hollis, Miriam Palacios-Callender, Nanci Frakich, Salvador Moncada. 2010. Inactivation of nitric oxide by cytochrome c oxidase under steady-state oxygen conditions. *Biochimica et Biophysica Acta (BBA) - Bioenergetics* **1797**:3, 371-377. [CrossRef]
15. Benjamin S. Rayner, Susan Hua, Tharani Sabaretnam, Paul K. Witting. 2009. Nitric oxide stimulates myoglobin gene and protein expression in vascular smooth muscle. *Biochemical Journal* **423**:2, 169-177. [CrossRef]
16. Daniela Laraspata, Vincenza Gorgoglione, Gianluigi La Piana, Valeria Palmitessa, Domenico Marzulli, Nicola Elio Lofrumento. 2009. Interaction of nitric oxide with the activity of cytosolic NADH/cytochrome c electron transport system. *Archives of Biochemistry and Biophysics* **489**:1-2, 99-109. [CrossRef]
17. Chris E. Cooper, Maria G. Mason, Peter Nicholls. 2008. A dynamic model of nitric oxide inhibition of mitochondrial cytochrome c oxidase. *Biochimica et Biophysica Acta (BBA) - Bioenergetics* **1777**:7-8, 867-876. [CrossRef]